Proposing PSS2B Stabilizer in Coordination with AVR of Brushless Excitation System to Enhance Stability of Khoy CCPP Steam Unit

J. Morsali, H. Morsali, R. Kazemzadeh, and M. R. Azizian

Abstract—**In order to achieve a much reliable generating unit, it is worthwhile to research on enhancing power system overall stability meticulously. Because of important role of Khoy combined cycle power plant (CCPP) in Azarbaijan power network from viewpoint of supplying crucial regional substations and contributing in power transfer to Turkey, also regarding this fact that in the steam unit there is no supplementary stabilizing controller, it is essential to improve the overall stability of the unit in a robust way to reduce the probability of the instabilities caused by large and small-signal perturbations. In this paper, a robust PSS2B stabilizer is proposed in coordination with automatic voltage regulator (AVR). Siemens brushless excitation, RG3, is modeled as a simplified form of the corresponding AC7B excitation system. The design problem is based on state space model of the steam unit and the coordination is concentrated on simultaneous adjustment of gains and time constants of the controllers using the PSO algorithm according to a multi-objective function. The eigenvalue analysis and Heffron-Phillips-based time domain simulations reveal greatly improvement in both transient and oscillation stabilities of the unit by utilizing our proposed PSS2B-AVR controllers. Clearly, this paper suggests equipping the unit with PSS2B-based industrial stabilizers as a retrofit in a refurbishment project.**

Index Terms—**AC7B excitation, PSS2B, coordinated design, PSO, steam unit, overall stability enhancement.**

I. Introduction

Power system overall stability can be explain regarding two different stability concepts. Transient stability means the ability of the power system to keep synchronism when exposed to severe transient disturbances. This stability can be affected mainly by contributing the automatic voltage regulator (AVR) unit. Small-signal or dynamic stability is the ability of system to return to a normal operating state, following a small disturbance. Investigations involving this concept usually involve the analysis of the linearized state space equations that define the power system dynamics [1], [2].

Local mode and inter-area mode oscillations are known as electromechanical (EM) modes. Local mode oscillation is associated with synchronous machines at a power plant, swinging jointly against a relatively large power system, within the frequency range of 0.8-2 Hz. Local oscillations are manifested in fluctuation of output variables of the synchronous generator, e.g. rotor angle, rotor speed, active power, and terminal voltage [3].

In order to damp EM oscillations and increase power systems dynamic stability, conventional power system stabilizer (CPSS) has been used routinely for many years in practical plants. Basic goal of the PSS installation is to apply a supplementary signal to the AVR of excitation system to produce additional electrical torque to damp out power oscillations effectively [4]. As the main duty of any PSS design is damping the oscillations, modal analysis based techniques such as residue method, participation factor, etc reveal that any signal that can affect the EM modes effectively, and also the oscillations are observable, can be a suitable candidate for the input signal of PSS. Two readily available local signals of the generator are the rotor speed and active power. Nowadays, the main trend in new industrial excitation control systems such as SIEMENS THYRIPOL, ALSTOM P320 AVR, BRUSH PRISMIC T20, ABB UNITROL 5000, EATON ECS2 100/PSS, Basler PSS-100 is to utilize the combination of aforementioned signals following IEEE 421.5 PSS2B recommendation to generate the stabilizing signal from the accelerating power to cover a wide range of oscillation frequencies in comparison with the CPSS structures [5]. The PSS2B is a little change of the PSS2A model introduced in [6] with three stage additional phase compensation blocks in the stabilizing part. It contains an internal filter to attenuate the shaft torsional oscillations as much as possible. This stabilizer is so built that is capable to work normally without any modification of steady state values of system voltage when a ramp change in the mechanical power occurred [7].

As a result of changes in power system topology after several years of operation, the parameters of excitation control system may deviate from optimum settings related to the unit initialization time. This matter can affect the unit stability locally and may reduce the capability of the generating unit. Also lacking assurance of accuracy of settings applied at the commissioning stages of the unit and needing to periodically check whether the parameters are optimum or not, lead to in several old steam units the PSS equipment is inactivated by the administer to avoid possible negative interactions between the AVR and PSS.

Khoy combined cycle power plant (CCPP) located in West Azarbaijan of Iran consists of two gas units in rating

Manuscript received November 8, 2011; revised June 12, 2012. This work was supported in part by the West Azarbaijan Elect. Power Gen. Management Co., Iran.

J. Morsali was with the Electrical Engineering Faculty, Sahand University of Technology, Tabriz, Iran, (e-mail: j_morsali@sut.ac.ir).

H. Morsali is with the Khoy Combined Cycle Power Plant, West Azarbaijan Elect. Power Gen. Management Company, Khoy, Iran, (e-mail: h1359.morsali@gmail.com).

R. Kazemzadeh and M. R. Azizian are with the Electrical Engineering Faculty, Sahand University of Technology, Tabriz, Iran, (e-mail: r.kazemzadeh@sut.ac.ir , azizian@sut.ac.ir).

Publisher Item Identifier S 1682-0053(12)1977

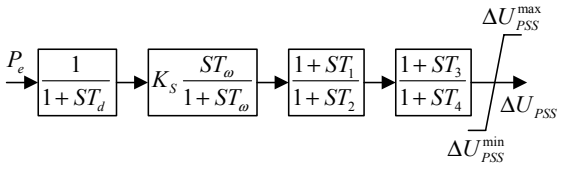

Fig. 1. Conventional P-type PSS.

of $2\times125\,\mathrm{MW}/13.8\,\mathrm{kV}$ and one steam unit in rating of $100\,\mathrm{MW}/10.5\,\mathrm{kV}$. Since it is sited in a particular location of the Azarbaijan power network from viewpoint of supplying important regional substations and contributing in power transfer through international transmission lines with Turkey country, it is necessary to enhance the unit overall stability to provide a much stable unit. However, in the present steam unit due to its old age there is no complementary stabilizing signal to have an impact on the RG3 AVR. It means that practically the PSS option is not regarded at all. A return to carefully analysis of the past events occurred in the steam unit discloses the high need to enhance the stability [8].

The Siemens RG3 system controls the excitation of the brushless generator. According to IEEE Standard 421.5, the corresponding model of the Siemens RG3 is IEEE type AC7B excitation system. It is composed of an ac alternator with rotating-diodes rectifier to provide the dc field requirement. If any supplementary stabilizer is applied, the PSS2B model is suitable [5].

Though a fast-acting AVR augments the power system transient stability, it can result in adverse effects on the damping torque and so on oscillation stability. However, the negative impact of the stabilizer on transient stability is not well known [9]. So uncoordinated design and control of the AVR and PSS installed on the same generator may cause destabilizing interactions even may restrict the operating power range of the generator. In order to minimize possible adverse interactions and improve the power system overall stability including the transient stability provided by the AVR and the oscillation stability achieved by the PSS, coordination between the controllers is essential [10].

This paper proposes robust coordinated design of integral of accelerating power-based stabilizer PSS2B and PI-AVR of the AC7B brushless ac excitation system. The design goal is to improve overall stability of the steam unit of Khoy CCPP under both large and small disturbances over a wide range of operating conditions. The design process is transformed into an optimization problem to minimize the eigenvalue-based multi-objective function in which the effects of controllers and 3 real operating conditions are considered concurrently. The PSO algorithm is utilized to optimize the adjustable parameters. The effectiveness of our proposed PSS2B-AVR coordinated controllers is evaluated by eigenvalue analysis and Heffron-Phillips-based time domain simulations in comparison with both assumed P-type CPSS-AVR pertains to prior works in literature and "No PSS" case related to current state of the steam unit.

II. Involved CPSS and PSS2B

In this part, the block models of considered P-type CPSS and PSS2B stabilizer are reviewed briefly.

A. P-Type CPSS

Fig. 1 shows the CPSS with active power input signal used vastly in old generating units such as in some full-option version of the Siemens RG3 excitation system. Time constant T_d may be employed to indicate the transducer time constant. Stabilizer gain and washout time constant are set by K_s and T_ω respectively. The washout reset block is a high-pass filter to eliminate the dc offset of PSS output. This property leads to the stabilizer not to modify the terminal voltage in steady state condition. The two blocks associated with T_1 to T_4 time constants provide required phase compensation characteristics [5].

The basic motivations to apply the electrical power as PSS input signal more readily instead of the speed are in view of the facts [11]:

- Large amounts of phase lead can be achieved.
- It is less susceptible to the noise troubles.
- It provides more satisfactory damping to local oscillation against the whole system.

In P-type CPSS design, it is assumed that the mechanical input power must be constant. So when forced mechanical power changes occur, this stabilizer issue unwanted output leads to large unacceptable variation in excitation and reactive power. Moreover, P-type CPSS affects mainly the local oscillations than inter-area [12]. These practical drawbacks and limitations influence on utilization of this stabilizer, thus many power-based stabilizers have been quickly replacing with the accelerating power-based designs. Nowadays the common practical tendency is toward utilizing IEEE type PSS2B stabilizer [5], [11]-[13].

B. IEEE Type PSS2B Stabilizer

Functional block diagram of the IEEE type PSS2B stabilizer is shown in Fig. 2. This modern stabilizer combines electrical power and rotor speed signals to make an equivalent speed signal that is proportional to the integral of accelerating power. From (1), the equivalent speed is equal to the integral of accelerating power divided by inertia constant $M=2H$. Thus if the speed signal can be evaluated, a stabilizer can be formed based on it. In PSS2B, mechanical power influences are regarded as really simple measurement from entirely electrical signals [11]

$$\Delta\omega_{eq}=\frac{1}{2H}\int(\Delta P_m-\Delta P_e)\mathrm{d}t=\frac{1}{M}\int\Delta P_{acc}\mathrm{d}t \qquad (1)$$

where P_m, P_e, and P_{acc} are the mechanical, electrical, and accelerating powers of the generator in per-unit, M and H are the inertia constant both in second, ω_{eq} is the equivalent angular speed in per-unit.

Two main parts of PSS2B are filter and stabilizing parts. Following the latest corresponded published works [3], [5], [7], the filter part parameters do not alter meaningfully based on the system conditions. These parameters are given in Appendix A. In Fig. 2, the parameters $(T_{W1}-T_{W4})$ and (T_6,T_7) represent washout and transducer time constants, respectively. Following the Appendix A values, the signal appearing at point A is proportional to the integral of mechanical power change and contains torsional component. It is passed through a low-pass filter to remove shaft torsional components. The time constants T_8 and T_9 of this filter are so selected to provide enough attenuation at all shaft torsional frequencies. If the torsional filter

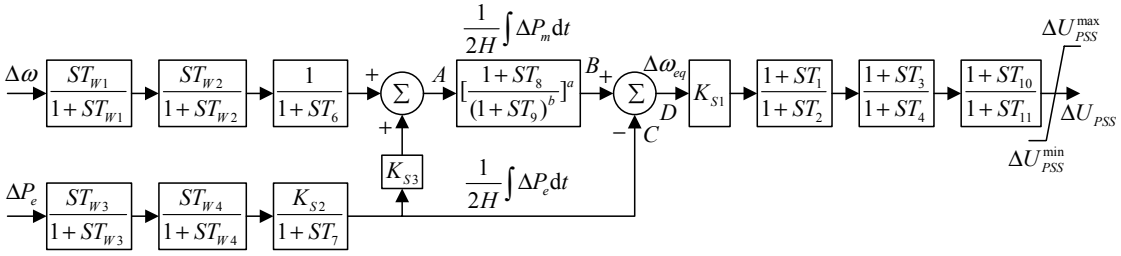

Fig. 2. IEEE type PSS2B stabilizer.

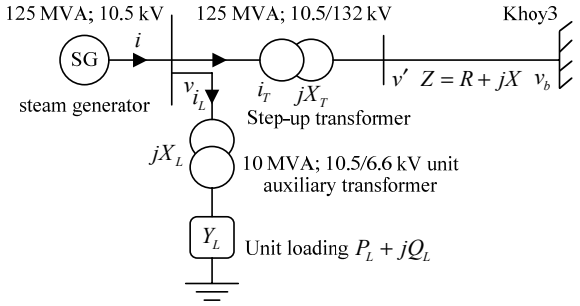

Fig. 3. Single line diagram of the steam unit.

parameters T_8, T_9, a, b fulfill $T_8/T_9 = b/a$, a ramp change in the mechanical input power is tolerable without any problems in normal work of the stabilizer in aspect of its zero output in the steady state condition [5], [12], [14]. It is much valuable because in practice, mechanical power changes are relatively slow even for fast valve movements. As seen in Fig. 2, the integral of accelerating power signal appeared in point D is made by synthesizing signals of points B and C. This filtered signal is then treated as the equivalent speed signal $\Delta\omega_{eq}$ for the stabilizing part. In order to maximize the contribution of the stabilizer in damping torque and help in the phase margin, three stage lead-lag compensators of PSS2B can easily compensate the phase lag in the oscillation frequency.

III. Power System Model

This section describes the generator and excitation system models of the steam unit. Also it gives the linearized model of involved single machine infinite bus (SMIB) power system.

A. Generator

In this study, the steam unit of Khoy power plant is considered as the test system shown in Fig. 3. The generator is connected to the Khoy3 unit substation through a step-up transformer and a short inter-unit transmission line. In this work it is considered that the involved RG3 excitation system is equipped with our proposed PSS2B stabilizer and the parameters are tuned optimally. In dynamic stability studies, the synchronous generator is commonly represented by the classical third order model comprising of (2) and (3) and the generator internal voltage (4) [1]. This model has been preferred in EM oscillation studies because of its simplicity and fast analysis. The inter-unit line impedance is $Z = R + jX$ and the generator terminal bus supplies the unit loads $P_L + jQ_L$ modeled as parallel admittance $Y_L = G + jB$ through the auxiliary unit transformer. The classical third order model is stated as [1], [15], [16]

$$\dot{\delta} = \omega_b(\omega - 1) \tag{2}$$

$$\dot{\omega} = \frac{1}{M}(P_m - P_e - D(\omega - 1)) \tag{3}$$

$$\dot{E}'_q = \frac{1}{T'_{do}}(E_{fd} - (x_d - x'_d)i_d - E'_q) \tag{4}$$

where D is the damping coefficient, δ, ω, and ω_b are the rotor angle, rotor speed, and synchronous speed $(2\pi f)$, respectively. E'_q is the machine internal voltage behind transient reactance, E_{fd} is the field voltage, T'_{do} is the field open circuit transient time constant, x_d and x'_d are d-axis reactance and d-axis transient reactance of the generator, respectively.

B. RG3 Excitation System

Fig. 4 shows the single line diagram of real generator excitation system, its interconnection with the voltage regulator and the other functions. The RG3 excitation system consists of three separate closed loop control systems. The basic function of control system 1 is the AVR with a subordinated current regulation. Control system 2 regulates the power factor and control system 3 manually controls the main exciter current regulator (ECR). All control systems are provided with a separate transistor chopper circuit. The transistor chopper circuits of the control systems are connected in parallel. The dc side of the transistor chopper circuit is connected via the surge arrester to the field winding of the main exciter. The excitation power for the transistor chopper circuit is provided from auxiliary winding of the generator and by the redundant battery during start-up and short circuit conditions [8]. Of the three separate control systems, it is the AVR that is normally in operation, as well during start-up as shut-down of the unit. During operation with the AVR, the other regulators continuously follow the reference value of the AVR, so that a changeover to manual operation is possible at every operation point. All limiters such as under excitation and over excitation, monitors and control functions are included in the excitation system and are processed by the 32-bit micro computer FM486. A proportional-integral (PI) controller is optimized at site to match the best operation condition of the generator. Fast acting limiters ensure safe operation at all conditions. Appendix B gives full data for our case study system [8], [17].

The IEEE type AC7B excitation system as shown in Fig. 5, is dual model of the RG3 that is composed of an ac alternator with rotating rectifiers to generate the dc field necessity. The gains K_{F1} and K_{F2} represent a high

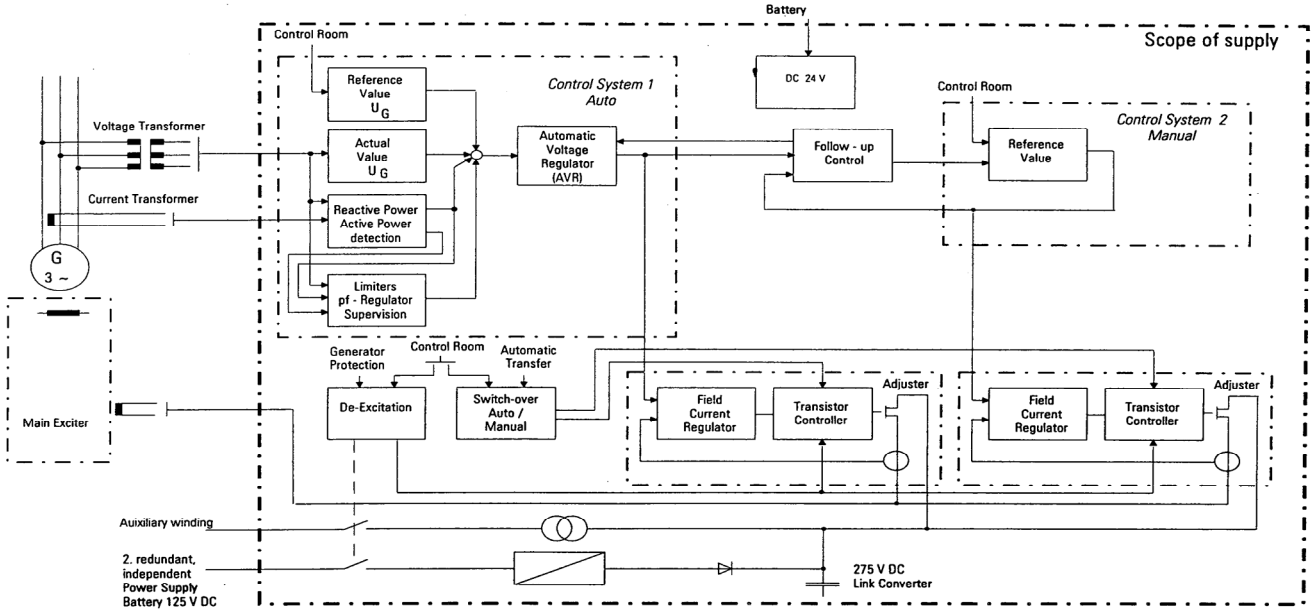

Fig. 4. Single line diagram of the RG3 excitation system for the steam unit [8].

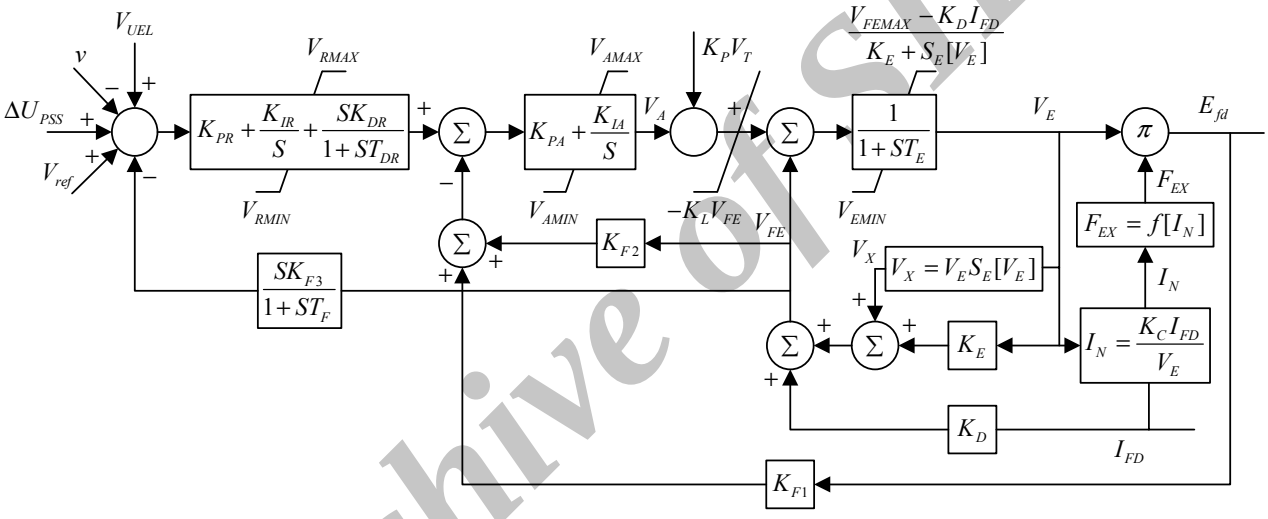

Fig. 5. IEEE type AC7B brushless excitation system model [5].

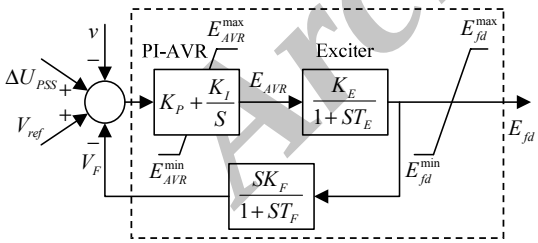

Fig. 6. Simplified model of the AC7B excitation system.

bandwidth interior loop regulating generator field voltage or exciter current. A fast exciter current limit V_{FEMAX}, is used to protect the field of the ac alternator. Another feedback loop (K_{F3}, T_F) is prepared for stabilization if a PI-AVR is implemented [5].

In this study, for simulating objectives, a simplified model of the AC7B is formed by considering an adjustable PI controller as the AVR model and a lag block associated with the natural delay of the exciter response because of its firing characteristic. According to simplified model shown in Fig. 6, the excitation system can be formulated as

$$\dot{E}_{fd} = -\frac{1}{T_E} E_{fd} + \frac{K_E}{T_E} E_{AVR} \tag{5}$$

$$\dot{V}_F = -\frac{1}{T_F} V_F - \frac{K_F}{T_E T_F} E_{fd} + \frac{K_F K_E}{T_F T_E} E_{AVR} \tag{6}$$

$$E_{AVR} = (K_P + \frac{K_I}{S})(U_{PSS} + V_{ref} - v - V_F) \tag{7}$$

where V_{ref} is the reference voltage, U_{PSS} is the supplementary signal from the PSS supplied to excitation system, v is terminal voltage, E_{AVR} is the PI-controller output signal (or exciter input signal), V_F is the output of the feedback from field voltage signal, K_I, K_P are the adjustable gains of the voltage regulator, K_E, T_E are the exciter gain and time constant, and K_F, T_F are feedback gain and time constant.

C. Steam Unit Linearized Model

The linearized expressions of the benchmark steam unit can be stated as [18]

$$\Delta\dot{\delta} = \omega_b \Delta\omega \tag{8}$$

$$\Delta\dot{\omega} = [\Delta P_m - \Delta P_e - D\Delta\omega]/M \tag{9}$$

$$\Delta\dot{E}'_q = [\Delta E_{fd} - k_3 \Delta E'_q - k_4 \Delta\delta]/T'_{do} \tag{10}$$

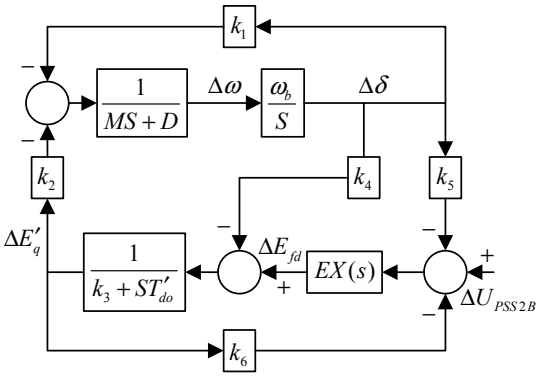

Fig. 7. Phillips-Heffron model of the steam unit equipped with PSS2B.

$$\Delta\dot{E}_{fd} = -\frac{1}{T_E}\Delta E_{fd} + \frac{K_E}{T_E}\Delta E_{AVR} \tag{11}$$

$$\Delta\dot{V}_F = -\frac{1}{T_F}\Delta V_F - \frac{K_F}{T_E T_F}\Delta E_{fd} + \frac{K_F K_E}{T_F T_E}\Delta E_{AVR} \tag{12}$$

$$\Delta E_{AVR} = (K_P + \frac{K_I}{S})(\Delta U_{PSS} + \Delta V_{ref} - \Delta v - \Delta V_F) \tag{13}$$

Since the generator is considered with fixed input power: $\Delta P_m = 0$. According to (8) to (13), primary state space variables of the benchmark power system are selected as

$$X = [\Delta\delta \quad \Delta\omega \quad \Delta E'_q \quad \Delta E_{fd} \quad \Delta E_{AVR} \quad \Delta V_F]^T \tag{14}$$

Fig. 7 illustrates block diagram of the linearized model of steam unit equipped with the PSS2B stabilizer. Although it is a linear model, suitable choice of the controller parameters can give effective damping to EM oscillations. Term $EX(s)$ is transfer function of excitation system shown inside the dashed block in Fig. 6.

The developed state space model of the steam unit with PSS2B can be obtained by assigning new state space variables according to Fig. 8 to the block model of the proposed PSS2B till the new state equations corresponding to these variables are added to system state matrix. Furthermore, the stabilizing signal ΔU_{PSS}, should be expressed in terms of the new state space variables to contribute the stabilizer effect in system state matrix.

IV. Implementation

In this part, the proposed controllers are designed and evaluated by eigenvalue analysis and time simulations.

A. Parameters of Proposed Controllers

In continuous of the paper, the parameters of proposed controllers (CPSS-AVR and PSS2B-AVR) are discussed.

1) CPSS & AC7B Excitation System

In this paper, regarding to Fig. 1 which is connected with the CPSS block model, the CPSS transducer and washout time constants (T_d, T_w), and the lag time constants of compensators (T_2, T_4), are given as: $T_d = 0.02\,\text{s}$, $T_w = 5\,\text{s}$, $T_2 = T_4 = 0.1\,\text{s}$ [16]. It is common in similar literature to predefine the lag time constants and adjust the corresponding lead ones to decrease the number of adjustable parameters and optimization burden. The upper and lower limits of the stabilizing signal are $\Delta U_{PSS}^{\max} = -\Delta U_{PSS}^{\min} = 0.2\,\text{p.u.}$ The gain (K_E) and time constant (T_E) of the exciter model in Fig. 6, also feedback parameters (K_F, T_F) are fixed to [5]: $K_E = 1$, $T_E = 1.1\,\text{s}$, $K_F = 0.212$, $T_F = 1.1\,\text{s}$. Finally, the CPSS gain (K_s) and lead time constants (T_1, T_3), and the proportional and integral gains of the AVR (K_P, K_I), remain to be optimized. These parameters are simultaneously tuned by PSO algorithm.

2) PSS2B & AC7B Excitation System

In this work, following Fig. 8 pertaining to allocation of new state variables to the PSS2B block model, the stabilizing signal is stated as

$$\Delta U_{PSS} = (1 - \frac{T_{10}}{T_{11}})x_{12} + \frac{T_{10}}{T_{11}}x_{11} \tag{15}$$

So the final state vector describing linear model of the power system equipped with PSS2B can be defined as

$$X = [\Delta\delta \quad \Delta\omega \quad \Delta E'_q \quad \Delta E_{fd} \quad \Delta E_{AVR} \quad \Delta V_F \quad \{\Delta x_i\}_{i=1}^{12}]^T \tag{16}$$

The filter part parameters including the P-channel and ω-channel transducers time constants (T_7, T_6), all washout time constants $(T_{w1}, T_{w2}, T_{w3}, T_{w4})$, torsional filter parameters a, b, T_8, T_9, also K_{s2} and K_{s3} are predetermined and are given in Appendix A. The lag time constants are considered as: $T_2 = 0.025\,\text{s}$, $T_4 = 0.02\,\text{s}$, $T_{11} = 0.033\,\text{s}$. The upper and lower limits of the stabilizer are $\Delta U_{PSS}^{\max} = -\Delta U_{PSS}^{\min} = 0.2\,\text{p.u.}$ From Fig. 6, the gain (K_E) and time constant (T_E) of the exciter model, also feedback parameters K_F, T_F have same values mentioned above. Therefore, the PSS2B gain (K_{s1}) and lead time constants (T_1, T_3, T_{10}), the proportional and integral gains (K_P, K_I) of the AVR, are concurrently optimized by PSO algorithm.

B. Objective Function

In order to obtain robust controllers, the adjustable parameters need to be optimized over various loading conditions concurrently. So in this work, an eigenvalue-based multi-objective function is utilized as [19]

$$J = \alpha\sum_{j=1}^{Nop}\sum_{\zeta_{i,j}\le\zeta_o}(\sigma_0 - \sigma_{i,j})^2 + \beta\sum_{j=1}^{Nop}\sum_{\sigma_{i,j}\ge\sigma_0}(\zeta_o - \zeta_{i,j})^2 \tag{17}$$

where $\sigma_{i,j}$ and $\zeta_{i,j}$ denote the real part and the damping ratio of the i th eigenvalue of the j th loading condition. Constants σ_0 and ζ_0 are chosen thresholds representing the desirable damping level. In this study, in order to take maximum advantage as much as possible from our proposed high-potential coordinated controllers, σ_0 and ζ_0 are chosen to be -2.0 and 0.3, respectively. These values are so selected that the execution time of the optimizing process remains sufficiently short. Parameters α and β are weighting factors which reflecting the contribution of each part in the objective function and have been fixed to 1 and 5, respectively. Parameter N_{op} is the total number of operating points considered together in optimization process to obtain robust controllers. In this paper, three operating points as light, nominal, and heavy loading conditions of the steam unit are considered. It is necessary to mention that only the unstable or lightly damped EM modes are relocated here. Briefly, the adjustable parameters of PSS2B and AVR are searched for optimal values simultaneously by PSO technique to improve the steam unit overall stability over different

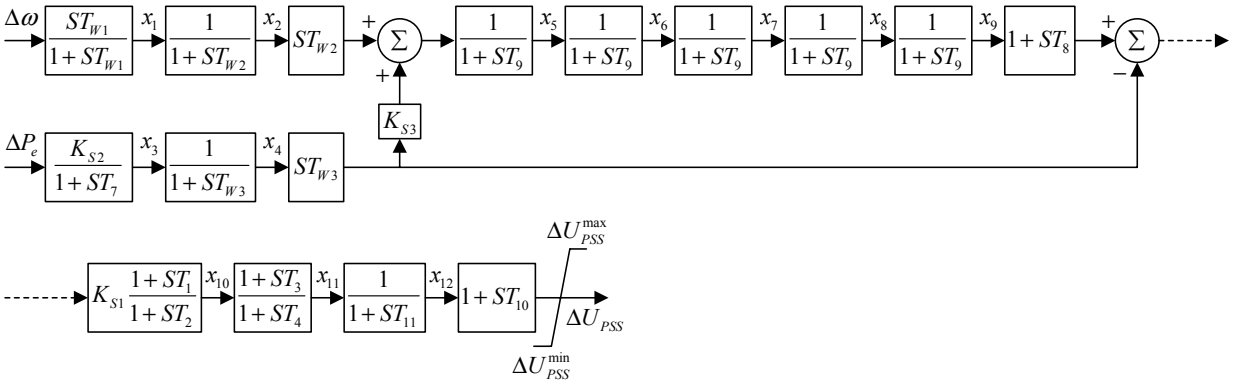

Fig. 8. Assign new state variables to dual-input PSS2B stabilizer.

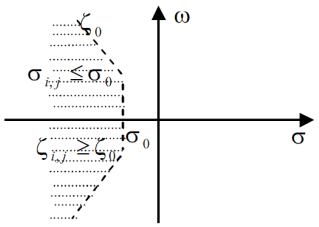

Fig. 9. Desired sector for repositioned eigenvalues.

operating conditions and under small and severe disturbances. For comparison purposes, CPSS is also designed in coordination with the excitation system in a similar way [20]. The design problem is to minimize J subject to constraints of tunable parameters

$$\begin{aligned} K_S^{\min} &\le K_S \le K_S^{\max} \\ K_{S1}^{\min} &\le K_{S1} \le K_{S1}^{\max} \\ T_1^{\min} &\le T_1 \le T_1^{\max} \\ T_3^{\min} &\le T_3 \le T_3^{\max} \\ T_{10}^{\min} &\le T_{10} \le T_{10}^{\max} \\ K_I^{\min} &\le K_I \le K_I^{\max} \\ K_P^{\min} &\le K_P \le K_P^{\max} \end{aligned} \tag{18}$$

Values of the lead time constants T_1, T_3 and T_{10} should set above the value of corresponding lag time constants T_2, T_4 and T_{11} to fully compensate the phase lag of the excitation system. The PSSs and AVR gains (K_S, K_{S1}, K_P, K_I) are optimized in range of (0.01, 10). According to the objective function, the aim of minimization of J is to shift the involved modes to the left half of s-plane inside the desired D-shaped sector for which, $\sigma_{i,j} \le \sigma_0$ and $\zeta_{i,j} \ge \zeta_0$ as depicted in Fig. 9 [19].

C. PSO Algorithm

Particle swarm optimization is a member of wide category of swarm intelligence methods which was introduced first in [21]. The PSO is a population-based search algorithm and recently it has acquired wide applications in engineering optimization problems. Fig. 10 shows the flowchart of the proposed PSO algorithm.

In the PSO, each particle is a candidate solution and the set of particles compose a population. Each particle is moving through an m-dimensional search space according to its adaptable velocity and adaptable position rule. The particle stores the position associated with its own best flying position it so far experienced in a personal memory called p_{best}. Also the best flying position ever visited by

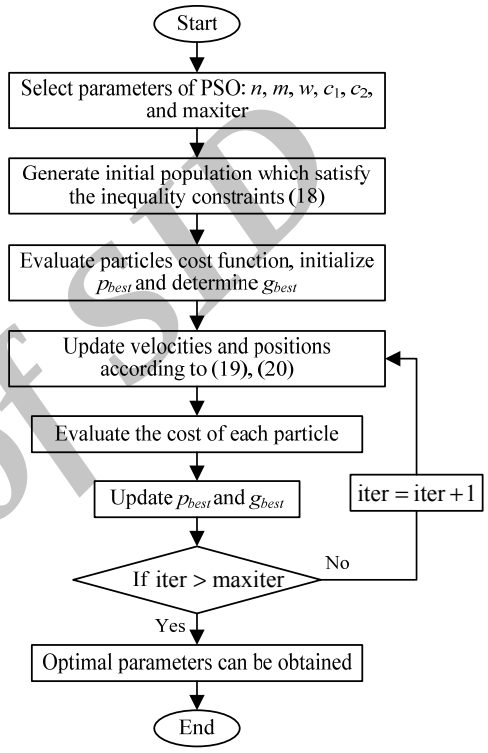

Fig. 10. Flowchart of the proposed PSO algorithm.

the group is stored, too and called g_{best} Variables p_{best} and g_{best} are updated in any iteration and particles try to enhance themselves by following features from theirvictorious peers. This concept can be formulated as [21], [22]

$$\begin{aligned} v_{j,k}^{(t+1)} &= w.v_{j,k}^{(t)} + c_1.r_1.(p_{best\,j,k} - x_{j,k}^{(t)}) \\ &\quad + c_2.r_2.(g_{best\,k} - x_{j,k}^{(t)}) \end{aligned} \tag{19}$$

$$\begin{aligned} x_{j,k}^{(t+1)} &= x_{j,k}^{(t)} + v_{j,k}^{(t+1)}, \\ j &= 1,2,\ldots,n \;,\; k = 1,2,\ldots,m \end{aligned} \tag{20}$$

where $x_j^{(t)}$ is current position of particle j at iteration t, n is the number of particles, m is the number of optimized parameters, w is the inertia weight factor which linearly decreases in each iteration, r_1 and r_2 are the uniformly distributed random numbers in the range (0,1), c_1 and c_2 constants are learning factors called the cognitive and social acceleration factors, respectively. These acceleration constants are responsible for varying the particle velocity towards p_{best} and g_{best}, respectively. Term $v_{j,k}^{(t)}$ is the kth dimension of current velocity vector of particle j at iteration t. The velocity vector is limited to maximum

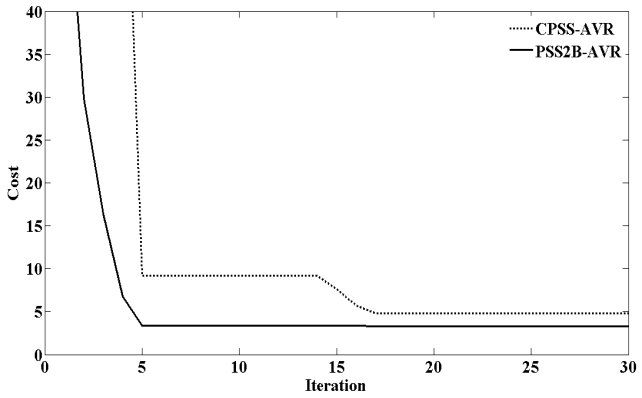

Fig. 11. Variations of the objective function.

TABLE I
PRACTICAL OPERATING CONDITIONS OF STEAM UNIT

	P (MW)	Q (MVAR)
Light loading	80	+15
Nominal loading	100	+20
Heavy loading	105	+25

TABLE II
OPTIMIZED PARAMETERS FROM PSO

	PSS2B-AVR		CPSS-AVR	
	PSS2B	AVR	CPSS	AVR
K_{S1}, K_S	8.1042	-	4.5039	-
K_I	-	4.0505	-	5.6541
K_P	-	5.1287	-	4.1314
T_1	0.1381	-	0.2341	-
T_3	0.1246	-	0.1325	-
T_{10}	0.1790	-	-	-

TABLE III
SYSTEM LOCAL MODES AND DAMPING RATIOS

Controller	Eigenvalue			Damping ratio		
	Light	Nominal	Heavy	Light	Nominal	Heavy
No PSS	$-0.3412 \pm 7.8721i$	$-0.3188 \pm 8.3833i$	$-0.1558 \pm 7.5617i$	0.0433	0.0380	0.0206
CPSS-AVR	$-1.9524 \pm 9.1287i$	$-1.9268 \pm 9.0397i$	$-1.8654 \pm 8.8791i$	0.2091	0.2085	0.2056
PSS2B-AVR	$-2.4143 \pm 7.1210i$	$-2.3584 \pm 7.0520i$	$-2.4256 \pm 7.1178i$	0.3211	0.3172	0.3226

values in positive and negative directions according to relation

$$v_{j,k}^{\max} = \gamma(x_{j,k}^{\max} - x_{j,k}^{\min}) \tag{21}$$

where γ is a chosen number in the interval (0,1) that controls the maximum permitted velocity of the particle. Parameter $\max iter$ in Fig. 10 is the maximum number of iterations, variable $iter$ is the current number of iteration, $w_{\max}$ and $w_{\min}$ are the initial and final weights, respectively.

D. Eigenvalue Analysis

The eigenvalues of linearized power system are quantitive indicators for steady state stability measurement. The EM modes are complex eigenvalues founded in the range of local oscillation frequencies. It can be concluded by participation factor method that in our discussed SMIB system there is only one EM mode of oscillation [23]. Following objective of the controller design procedure, the regarded minimum damping ratio and real part should be satisfied. In the present paper, to achieve the robust PSS2B stabilizer, three practical operating conditions are considered in design procedure concurrently as shown in Table I. Light loading condition is related to situation that the both involved gas units of Khoy CCPP operate in minimum power generation. Normal loading condition pertains to case that both gas units work in base load and the steam unit is in continuous operation situation. Heavy loading condition deals with generation of the steam unit over nominal rate that often occurs in winter season due to high efficiency of gas units in cold weather conditions.

In optimization stage, at first some executions have been done with various values of PSO parameters. The final algorithm parameters for MATLAB-based proposed PSO program are selected as: $n = 30$, $\max iter = 30$, $w_{\min} = 0.4$, $w_{\max} = 0.9$, $c_1 = c_2 = 2$, and $\gamma = 0.1$. These parameters should be chosen attentively for successful consequence of the algorithm. By try and error method, it has been realized that these values satisfy all simulation issues of this paper. Table II shows the optimal parameters of the both proposed coordinated controllers. Fig. 11 illustrates the convergence rate of the objective function when the controllers are tuned. From Fig. 11, it is observed that the cost value is less than for PSS2B equipped system which indicates better performance of PSS2B-AVR design in fulfilling our goals. From the objective function, it is evident that as much as possible the damping ratios and damping constants of the relocated eigenvalues are close to the desired thresholds or inside the proposed sector, a small cost of the design can be obtained.

In Table III, system local modes and damping ratios in cases of without and with coordinated controllers are summarized using the modal analysis based mode shapes and participation factors associated with rotor speed and rotor angle signals [23], [24]. The damping ratio seems to be a suitable criterion for eigenvalue stability characteristic. From Table III, the steam unit in absence of any PSS is near to instability at heavy loading condition as a result of the low damping ratio. Also the system has weakly damped EM in light loading and damping ratio of fewer than 5% in nominal condition, too. These notices mean that a severe disturbance in system can lead to heavy oscillations that continue for some seconds or minute to be damped or may even cause instability. From Table III, it can be understood that the PSS2B stabilizer is more capable than CPSS to move the oscillation mode inside the desired sector. In other words, the proposed PSS2B-AVR coordinated controllers improve greatly the system damping indices since the damping ratio and damping coefficient of the EM mode have been significantly increased.

E. Time Domain Simulations

It has been stated in [23] that the linear controllers proposed for power system oscillation stability enhancement should perform satisfactorily under large disturbances. Thus, the robustness and effectiveness of the proposed controllers are evaluated under both large-signal transient disturbance and two small-signal perturbations in the MATLAB/SIMULINK environment based on the Heffron-Phillips model. However, the figures are depicted approximately in tangible values instead of per-unit of deviations. This helps us to deal with actual values and technical interpretations.

The severe disturbance is a 3-phase 6-cycle short circuit on the Khoy3 unit substation without inter-unit line outage for the nominal loading condition. The two small-signal perturbations are a step decrease of 5% in the reference voltage ΔV_{ref} at the instant of 10.0 s and a step decrease of 5% in the mechanical input power ΔP_m at the instant of 10.0 s for the light and heavy loading conditions, respectively. The time 10.0 s is selected to ensure that the initial transient conditions of the system have been passed. The rotor angle, speed, machine active power, terminal voltage, and PSS stabilizing signal responses have been shown in Figs. 12(a), 12(b), 12(c), 12(d), and 12(e), respectively. After a glance to these illustrations, it can be noticed that the PSS2B-equipped model shows greater damping characteristics than for CPSS counterpart and superior results in comparison to "No PSS" case in term of decrease in overshoot, undershoot and settling time of depicted outputs.

According to Fig. 12(a), rotor angle in "No PSS" case swings highly over ten seconds with low settling time. In presence of CPSS controller, the settling time decreases somewhat though, the overshoot and undershoot are large still which is unsatisfactory in oscillation stability. The settling time is an important stability index to evaluate the capability of the system to return to normal operating condition as soon as possible. In the PSS2B-AVR case, the rotor angle response is much desirable as it has been suppressed remarkably with the lowest overshoot, undershoot and settling time. In "No PSS" case of Fig. 12(b), due to the severe disturbance, rotor speed oscillates with a very large deviation from the steady state value. This is serious situation and may lead to activate some alarms such as over speed protection even trip the unit directly. From Fig. 12(b), it is clear that our proposed coordinated controllers give greater damping to the rotor speed oscillations than the AVR-CPSS since the speed swing has been damped quickly with the lowest overshoot and undershoot among others. Following "No PSS" case of Fig. 12(c), the short circuit fault immediately impacts on active power generation in megawatt ranges that can bring about unit trip. Optimistically, undesirable power oscillations remain for a long time on system output after clearing the faulty condition. The conventional coordination increases the damping characteristics to some extent though, it is not satisfactory in viewpoint of the settling time index. As seen in Fig. 12(c), the settling time has diminished by applying the proposed PSS2B stabilizer. Thus, the greatest damping in active power oscillation has been obtained by employing the PSS2B-AVR. It can be

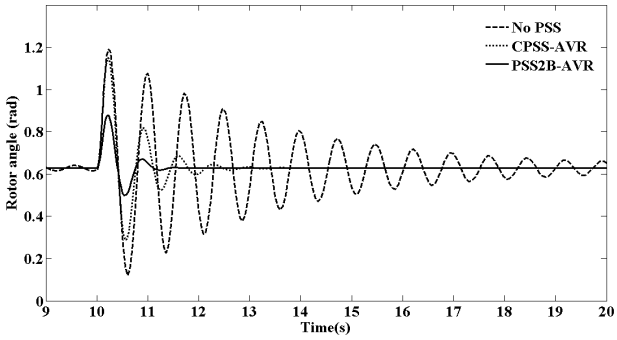

(a)

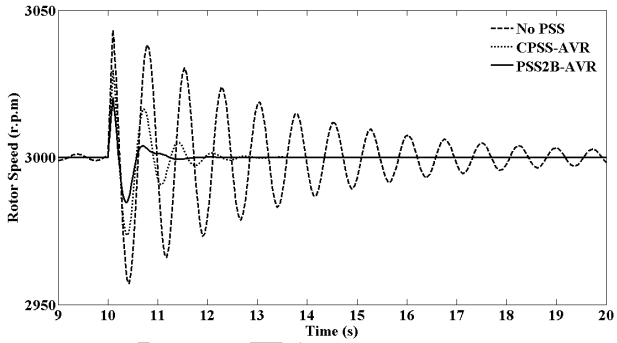

(b)

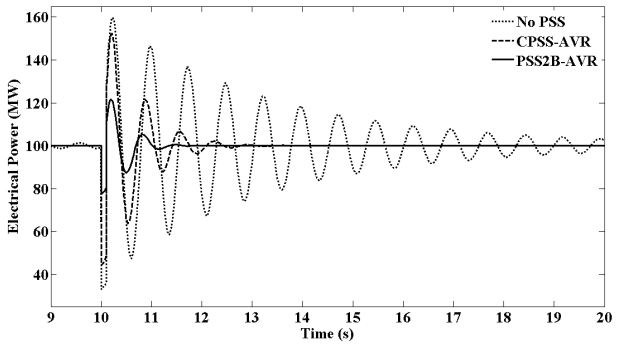

(c)

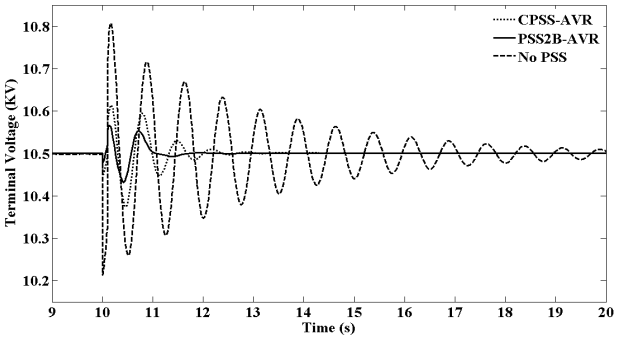

(d)

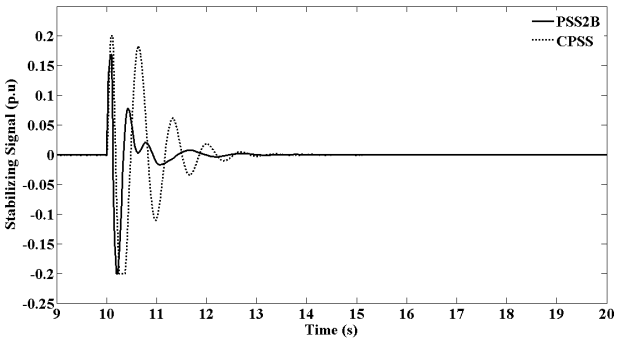

(e)

Fig. 12. System nominal responses for the large disturbance, (a) rotor angle, (b) rotor speed, (c) machine active power, (d) terminal voltage, and (e) stabilizing signal.

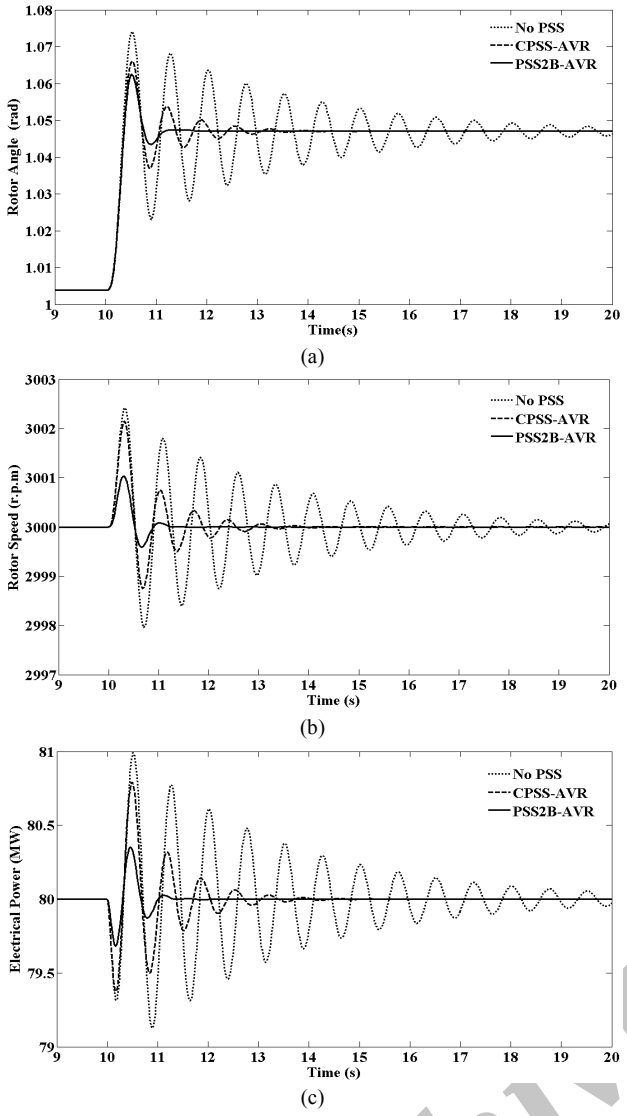

Fig. 13. System light responses for reference voltage disturbance, (a) rotor angle, (b) rotor speed, and (c) machine active power.

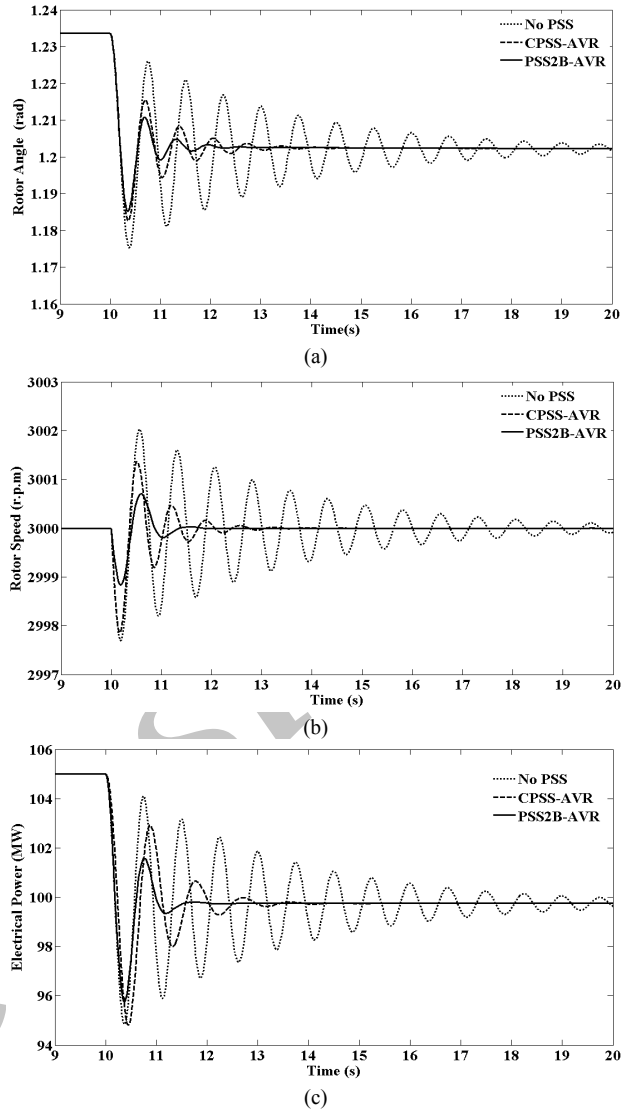

Fig. 14. System heavy responses for mechanical power disturbance, (a) rotor angle, (b) rotor speed, and (c) machine active power.

seen from Fig. 12(d) that simulated fault affects the terminal voltage to oscillate severely which is unwilling. With the AVR-CPSS controllers, the overshoot and undershoot of voltage signal have decreased though, the settling time is large and undesirable. The designed PSS2B stabilizer can decrease the voltage oscillation range to a few Volts that settles in a second. The Fig. 12(e) illustrates stabilizing signals of the CPSS and PSS2B stabilizers. Both stabilizers are limited to upper and lower bounds.

Figs. 13 and 14 show the light and heavy loading responses of the rotor angle, rotor speed, and active power signals for the perturbations in the reference voltage and mechanical input power, respectively. From Figs. 13(a) and 14(a), the rotor angle in "No PSS" case oscillates severely with low settling time. As seen in the figures, the reference voltage disturbance under light loading condition cause increase in the rotor angle whereas the mechanical power disturbance under heavy loading condition result in decrease in the rotor angle. With applying the AVR-CPSS controllers, rotor angle profiles of the both loading conditions have been improved though, the oscillations have been damped very weakly with long settling time and high overshoot and undershoot that are unsatisfactory.

By applying our proposed controllers, great damping enhancement has been taken place in outputs in figure of reduce in settling time, overshoot and undershoot of the rotor angle signal in comparison with the AVR-CPSS equipped system profiles. From Figs. 13(b) and 14(b) it is obvious that the speed oscillations in the "No PSS" case have diminished poorly for both light and heavy loading conditions. The speed swings have been mitigated to some degree by utilizing the AVR-CPSS controllers. According to these figures, the PSS2B-equipped model has shown the greatest results in damping the speed oscillations. As shown in Figs. 13(c) and 14(c), the active power has oscillated for a long time in "No PSS" case. The conventional coordination can weaken the oscillations to some extent though, the long settling time is unacceptable still. It is evident that in order to damp active power oscillations effectively, AVR-PSS2B controllers are the best choice.

From all simulation results we can conclude that the AVR-PSS2B coordination has shown greater damping characteristics than the CPSS-AVR to enhance the unit overall stability. This outcome is in confirmation with the eigenvalue analysis result.

F. Real Plant Events

Prior to this work, we have fulfilled a full investigation in connection with the AVR and excitation system of the steam unit, RG3, reported in [25]. Although the gathered information from the manufacturer data sheets has been utilized in our simulations as much as needed, the unit recorded data extracted from the magneto optical disk (MOD) were not suitable to be compared with our simulations. Because, due to old version of the existing event recorders, we could not find any similar 3-phase fault recently happened in the specified point of the unit.

V. CONCLUSIONS

This paper has proposed robust coordinated design of the accelerating power stabilizer PSS2B and PI-AVR of the AC7B brushless excitation system to decrease the EM oscillations and increase significantly the stability of Khoy CCPP steam unit. Since no PSS equipment has been regarded in the unit and essential attention to enhance the stability indices was needed, we have tried to simulate the dynamic model of the unit in minimum data mainly focused on employing PSS2B as an industrial stabilizer that is capable to work successfully as retrofit in refurbished units as well as being incorporated into new systems. For another good point of this work, we have also tried to find corresponding IEEE standard excitation system for modeling of the Siemens RG3 system to employ in the coordinated design problem. The performance of our proposed PSS2B-AVR coordinated controllers has been compared with CPSS-AVR and also current condition of the simulated steam unit. The eigenvalues analysis has demonstrated that our controllers are capable to shift the EM mode to the desired area completely and improve damping characteristics of the poorly damped modes. The results of time domain simulations performed under various small-signal and severe disturbances have revealed the superior effectiveness of our PSS2B-AVR controllers to damp the unit EM oscillations. Distinctly, this paper suggests planning an industrial PSS2B stabilizer as retrofit in coordination with the RG3 system to enhance steam unit overall stability.

APPENDIX A

PSS2B filter part data

$T_{W1} = T_{W2} = T_{W3} = T_7 = 10\,\text{s}$, $T_{W4} = 0$, $T_6 \approx 0$

$K_{S3} = 1$, $K_{S2} = T_7/(2H)$, $a = 1$, $b = 5$

$T_8 = 0.5$, $T_9 = 0.1$

APPENDIX B

Full data for Khoy steam unit is presented in Table B.

TABLE B
KHOY CCPP STEAM UNIT DATA [8], [17]

Main generator data	
Generator type	Siemens TLRI 100/36
Excitation system	Brushless RG3-DF
PSS option	Not regarded
Rated apparent power	$S_n = 125\,\text{MVA}$
Rated active power	$P_e = 100\,\text{MW}$
Rated line voltage	$V = 10.5\,\text{kV}$
Rated speed	r.p.m. = 3000
Frequency	$f = 50\,\text{Hz}$
Inertia in minimum data	$H = 4.31\,\text{sec}$
Transient time constant	$T'_{do} = 6.1479\,\text{sec}$
D-axis transient reactance	$X'_d = 0.26\,\text{p.u.}$
D-axis reactance	$X_d = 2.11\,\text{p.u.}$
Q-axis reactance	$X_q = 1.73\,\text{p.u.}$
Rated power factor	$\cos\varphi = 0.8$
Step-up transformer	
Rated power	125 MVA
Rated line voltage	132 kV
Base impedance	$Z_{bT} = 139.39\,\Omega$
Short circuit reactance	$X_T = 0.124\,\text{p.u.}$
Unit auxiliary transformer	
Rated power	10 MVA
Rated line voltage	10.5 KV
Base impedance	$Z_{bL} = 11.03\,\Omega$
Short circuit reactance	$X_L = 0.07\,\text{p.u.}$
Inter-unit line impedance	$Z = 0.104 + j\,0.532\,\text{p.u.}$
Unit loading	$P_L + jQ_L = 0.024 + j\,0.0184$

APPENDIX C

Power system linearized model:

From Fig. 3 it can be written

$$v_b = v - [R + j(X + X_T)]i_T \quad \text{(C-1)}$$

$$i_L = [G + j(B - \frac{1}{X_L})]v \quad \text{(C-2)}$$

$$i = i_L + i_T \quad \text{(C-3)}$$

after substituting (C-1), (C-2) into (C-3), it can be written as

$$i_d + ji_q = \frac{v_d + jv_q}{G + j(B - \frac{1}{X_L})} + \frac{v_d + jv_q - (v_{bd} + jv_{bq})}{R + j(X + X_T)} \quad \text{(C-4)}$$

substituting v_d , v_q , v_{bd} , v_{bq} into (AC-4) leads to

$$i_d + ji_q = \frac{x_q i_q + j(E'_q - x'_d i_d)}{G + j(B - \frac{1}{X_L})} + \frac{x_q i_q + j(E'_q - x'_d i_d) - (v_b \sin\delta + jv_b \cos\delta)}{R + j(X + X_T)} \quad \text{(C-5)}$$

after separating (C-5) to real and imaginary parts, then linearizing them at the nominal loading condition and solving together, Δi_d and Δi_q can be obtained as

$$\Delta i_d = c_1 \Delta\delta + c_2 \Delta E'_q \quad \text{(C-6)}$$

$$\Delta i_q = c_3 \Delta\delta + c_4 \Delta E'_q \quad \text{(C-7)}$$

the constants $c_1 - c_4$ are terms based on system parameters and initial conditions. The linearized d-axis and q-axis components of the terminal voltage can be written as

$$\Delta v_d = x_q \Delta i_q \tag{C-8}$$

$$\Delta v_q = \Delta E'_q - x'_d \Delta i_d \tag{C-9}$$

the linearized terminal voltage can be written as

$$\Delta v = (\frac{v_{d0}}{v_0})\Delta v_d + (\frac{v_{q0}}{v_0})\Delta v_q \tag{C-10}$$

substituting (C-8), (C-9) into (C-10) leads to

$$\Delta v = (\frac{v_{d0}}{v_0} x_q)\Delta i_q - (\frac{v_{q0}}{v_0} x'_d)\Delta i_d + \frac{v_{q0}}{v_0}\Delta E'_q \tag{C-11}$$

substituting (C-6), (C-7) into (C-11) leads to

$$\Delta v = k_5 \Delta\delta + k_6 \Delta E'_q \tag{C-12}$$

from (4), linearized internal voltage can be written as

$$(1 + ST'_{do})\Delta E'_q = \Delta E_{fd} - (x_d - x'_d)\Delta i_d \tag{C-13}$$

substituting (C-6) into (C-13) leads to

$$(k_3 + ST'_{do})\Delta E'_q = \Delta E_{fd} - k_4 \Delta\delta \tag{C-14}$$

the linearized active power can be written in form of

$$\Delta P_e = v_{d0}\Delta i_d + i_{d0}\Delta v_d + v_{q0}\Delta i_q + i_{q0}\Delta v_q \tag{C-15}$$

substituting (C-8), (C-9) into (C-15) leads to

$$\begin{aligned}\Delta P_e &= (v_{d0} - x'_d i_{q0})\Delta i_d \\ &+ (v_{q0} + x_q i_{d0})\Delta i_q + i_{q0}\Delta E'_q\end{aligned} \tag{C-16}$$

substituting (C-6), (C-7) into (C-16) leads to

$$\Delta P_e = k_1 \Delta\delta + k_2 \Delta E'_q \tag{C-17}$$

the constants $k_1 - k_6$ are expressions of system parameters and initial conditions. Note that the second zero subscript is used to identify the initial values.

REFERENCES

[1] Y. N. Yu, *Electric Power System Dynamics*, New York: Academic Press, 1983.

[2] P. W. Sauer and M. A. Pai, *Power System Dynamics and Stability*, New Jersey: Prentice Hall, 1997.

[3] G. Rogers, *Power System Oscillations*, Boston: Kluwer Academic, 2000.

[4] E. V. Larsen and D. A. Swann, "Applying power system stabilizers: part I: general concepts," *IEEE Trans. Power Apparatus Syst.*, vol. 100, no. 6, pp. 3017-3024, Jun. 1981.

[5] *IEEE Recommended Practice for Excitation System Models for Power System Stability Studies*, IEEE Standard 421.5-2005 (Revision of IEEE Standard 421.5-1992), Apr. 2006.

[6] *IEEE Recommended Practice for Excitation System Models for Power System Stability Studies*, IEEE Standard 421.5-1992, Aug. 1992.

[7] A. Murdoch, S. Venkataraman, and R. A. Lawson, "Integral of accelerating power type PSS, part II, field testing and performance verification," *IEEE Trans. Energy Conv.*, vol. 14, no. 4, pp. 1664-1672, Dec. 1999.

[8] Ministry of Energy, Iran Power Development Co. (IPDC), and MAPNA Co., *Project: Khoy CCPP, Generator Excitation System RG3-DF Automatic Voltage Regulator, Operation & Maintenance Manual*, vol. 1, 1992.

[9] G. J. W. Dudgeon, W. E. Leithead, A. Dysko, J. O'Reilly, and J. R. McDonald, "The effective role of AVR and PSS in power systems: frequency response analysis," *IEEE Trans. Power Sys.*, vol. 22, no. 4, pp. 1986-1994, Nov. 2007.

[10] A. Dysko, W. E. Leithead, and J. O'Reilly, "Enhanced power system stability by coordinated PSS design," *IEEE Trans. on Power Systems*, vol. 25, no. 1, pp. 413-422, Feb. 2010.

[11] F. P. De Mello, L. N. Hannett, and J. M. Undrill, "Practical approaches to supplementary stabilizing from accelerating power," *IEEE Trans. Power Apparatus Syst.*, vol. 97, no. 5, pp. 1515-1522, Sep. 1978.

[12] G. R. Berube, L. M. Hajagos, and R. Beaulieu, "Practical utility experience with application of power system stabilizers," in *Proc. IEEE PES Summer Meeting 1999,* vol. 1, pp. 104-109, Edmonton Alberta, Canada, Jul. 1999.

[13] J. P. Bayne, D. C. Lee, and W. Watson, "A power system stabilizer for thermal units based on derivation of accelerating power," *IEEE Trans. Power Apparatus Syst.*, vol. 96, no. 6, pp. 1777-1783, Nov. 1977.

[14] Z. Tecec, V. Cesic, and I. Petrovic, "Some issues of microprocessor-based power system stabilizer implementation," in *Proc. Mediterranean Conf. Control & Automation, MED'07*, 6 pp., Athens-Greece, 27-29 Jun. 2007.

[15] Y. L. Abdel-Magid and M. A. Abido, "Robust coordinated design of excitation and TCSC-based stabilizers using genetic algorithms," *Elect. Power Syst. Res.*, vol. 69, no. 2-3, pp. 129-141, 2004.

[16] M. A. Abido, "Pole placement technique for PSS and TCSC-based stabilizer design using simulated annealing," *Elect. Power Energy Syst.*, vol. 22, no. 8, pp. 543-554, 2000.

[17] Ministry of Energy, Iran Power Development Co. (IPDC), and MAPNA Co., *Project: Khoy CCPP, Generator/Transformer, Protection Relays Setting Calculation Manual*, 1992.

[18] H. F. Wang and F. J. Swift, "A unified model for the analysis of FACTS devices in damping power system oscillations, I, single-machine infinite-bus power systems," *IEEE Trans. on Power Delivery*, vol. 12, no. 2, pp. 941-946, Apr. 1997.

[19] Y. L. Abdel-Magid and M. A. Abido, "Optimal multiobjective design of robust power system stabilizers using genetic algorithms," *IEEE Trans. Power Sys.*, vol. 18, no. 3, pp. 1125-1132, Aug. 2003.

[20] A. D. Falehi, M. Rostami, and H. Mehrjardi, "Transient stability analysis of power system by coordinated PSS-AVR design based on PSO technique," *Engineering*, vol. 3, no. 5, pp. 478-484, May 2011.

[21] J. Kennedy and R. Eberhart, "Particle swarm optimization," in *Proc. IEEE Int. Conf. on Neural Networks, Proc.,* vol. 4, pp. 1942-1948, Perth, Australia, Nov./Dec. 1995.

[22] J. Kennedy, R. C. Eberhart, and S Y. Shi, *Swarm Intelligence*, San Francisco: Morgan Kaufmann, 2001.

[23] P. Kundur, *Power System Stability and Control*, New York: McGraw-Hill, 1994.

[24] Y. Y. Hsu and C. L. Chen, "Identification of optimum location for stabiliser applications using participation factors," *IEE Generation, Transmission, and Distribution*, vol. 134, no. 3, pp. 238-244, 1987.

[25] H. Morsali and J. Morsali, *Investigation of the Excitation System and AVR of the Khoy CCPP-Steam Unit*, Technical Report by the Operation Group of the Khoy CCPP, West Azarbaijan Electric Power Generation Management Company, Khoy, Iran, 2010. (in Persian)

Javad Morsali was born in Khoy, Iran, in 1986. He received his B.Sc. and M.Sc. degrees, both in electrical power engineering, from the University of Tabriz and Sahand University of Technology, in 2008 and 2011, respectively. He is the Ph.D. student in electrical power engineering at the Tabriz University, since 2012.

He has contributed in some projects about generator excitation control systems of Khoy CCPP. He has authored and co-authored more than 8 technical reports and conference papers. His research interests include power system dynamics and stability, flexible ac transmission system (FACTS), automatic generation control (AGC), and power system restructuring.

Hossein Morsali was born in Khoy, Iran, in 1981. He received his Associate Degree and B.Sc. degree both in electrical power engineering from the Islamic Azad University of Abhar, in 2005 and 2009, respectively. He has been employed in the West Azarbayjan Electric Power Generation and Management Company in 2007 and has worked at Orumieh CCPP from 2007 to 2009. He is with the Operation Group of Khoy CCPP, since 2009.

He has accomplished some technical reports by researching on excitation control systems of Khoy CCPP. He has been the co-author of some conference articles. His research interests include power plant excitation control systems, generation, operation, and its protection.

Rasool Kazemzadeh received his B.Sc. and M.Sc. degrees both in Electrical Power Engineering from Iran University of Science and Technology, and Tabriz University, Iran, in 1989 and 1992 respectively, and the Ph.D. degree in Electrical Engineering from Universite de Franche Comte, France, in 2005. He is currently an Assistant Professor at Sahand University of Technology, Tabriz Iran.

His research interest is electrical power systems, distribution networks, power electronics application on power systems, and distributed generation.

Mohammad Reza Azizian received the B.Sc. and M.Sc. degrees in electrical engineering from Tabriz University, Tabriz, Iran, in 1988 and 1991, respectively, and the Ph.D. degree in electrical engineering from the Brno University of Technology, Brno, Czech Republic, in 2003.

From 1991 to 1999, he worked as a research assistant at Sahand University of Technology, Tabriz, Iran, where he is now an assistant Professor. His teaching activities include Electrical Machinery, Electrical Drives and power Electronics. He has carried out research in the field of motion control, application of static converters, parameter estimation of BLDC and induction motor drives, design and implementation of power converters.